Biochemistry **1996,** *35,* 15447−15460 15447

Fourier Transform Infrared Difference Study of Tyrosine$_D$ Oxidation and Plastoquinone Q_A Reduction in Photosystem II[†]

Rainer Hienerwadel, Alain Boussac,[‡] Jacques Breton, and Catherine Berthomieu*

Section de Bioénergétique, CEA-Saclay, and URA CNRS 2096, 91191 Gif-sur-Yvette Cedex, France

Received August 6, 1996; Revised Manuscript Received September 30, 1996[⊗]

ABSTRACT: Two redox active tyrosines are present in the homologous polypeptides D1 and D2 of photosystem II (PS II). Tyr$_Z$ (D1−161) is involved in the electron transfer reactions resulting in oxygen evolution, while Tyr$_D$ (D2−160) usually forms a dark-stable radical. In Mn-depleted PS II, Tyr$_D^\bullet$ can be slowly reduced by exogenous reductants. Charge separation then results in the oxidation of Tyr$_D$ and Tyr$_Z$ and the reduction of the primary electron acceptor Q_A. The semiquinone Q_A^- can be reoxidized by oxidants like ferricyanide. In the present work, experimental conditions leading to the generation of pure Q_A^-/Q_A or Tyr$_D^\bullet$/Tyr$_D$ FTIR difference spectra have been optimized. Therefore, single-turnover flashes or short illuminations were performed on PS II samples in the presence of exogenous reductants or oxidants. The Q_A^- and Tyr$_D^\bullet$ radicals were generated with high yield and with a lifetime of several seconds or minutes allowing averaging of FTIR difference spectra with high signal to noise ratio. Both Q_A^- formation and contributions at the electron donor side of PS II were monitored by EPR spectroscopy. In PS II samples at pH 6 in the presence of PMS, NH_2OH, and DCMU, EPR measurements show that Q_A^- is formed with high yield upon a 1 s illumination at 10 °C, while no radical from the electron donor side of PS II is detected. Therefore the Q_A^-/Q_A FTIR spectrum obtained in these conditions shows only vibrational changes due to Q_A reduction in PS II. In contrast, a similar spectrum was recently interpreted in terms of dominant contributions from Chl$^+$/Chl signals [MacDonald, G. M., Steenhuis, J. J., & Barry, B. A. (1995) *J. Biol. Chem. 270,* 8420−8428], although the contribution from the electron acceptor Q_A was not quantified. In particular, it is shown here that the large positive signal at 1478 cm^{-1} is due to the Q_A^- state and not to a Chl$^+$ mode. This band is not downshifted upon ^{15}N-labeling of spinach PS II membranes within the ±1 cm^{-1} accuracy of the method and is therefore tentatively assigned to the ν(C$\cdots$O) mode of the plastosemiquinone Q_A^-. Also unchanged upon ^{15}N-labeling, signals at 1644 and/or1630 cm^{-1} are possible candidates for the ν(C=O) mode(s) of neutral Q_A in PS II. The Tyr$_D^\bullet$/Tyr$_D$ FTIR spectrum is recorded at 4 °C on Tris-washed PS II membranes from spinach at pH 6 in the presence of phosphate, formate, and ferricyanide. EPR experiments performed on these samples show that almost all Tyr$_D^\bullet$ is formed upon a 1 s illumination at 4 °C and that Tyr$_D^\bullet$ is then reduced within 12 min in the dark. No contributions from Tyr$_Z^\bullet$ or Q_A^- are detected 2 s after illumination. It is thus possible to optimize experimental conditions to record the FTIR difference spectrum only due to Tyr$_D$ photooxidation in PS II-enriched membranes of spinach. The Tyr$_D^\bullet$/Tyr$_D$ FTIR spectrum is compared to a cresol$^\bullet$/cresol FTIR difference spectrum obtained by UV irradiation at 10 K of cresol at pH 8. The spectral analogies observed between the *in vivo* and *in vitro* spectra recorded either in H_2O or in D_2O suggest that IR modes of Tyr$_D$ contribute at 1513 and 1252 cm^{-1}. These frequencies are characteristic of a protonated tyrosine. A positive signal is observed at 1506 cm^{-1} for cresol$^\bullet$ and at 1504 cm^{-1} for the Tyr$_D^\bullet$ state. This suggests contribution of the Tyr$_D^\bullet$ side chain at 1504 cm^{-1}. A band at 1473 cm^{-1} was previously assigned to the ν(CO) mode of Tyr$_D^\bullet$ [MacDonald, G. M., Bixby, K. A., & Barry, B. A. (1993) *Proc. Natl. Acad. Sci. U.S.A. 90,* 11024−11028]. In contrast, no positive signal is observed at 1473 cm^{-1} in the Tyr$_D^\bullet$/Tyr$_D$ FTIR difference spectrum presented here. The Tyr$_D^\bullet$/Tyr$_D$ spectrum also shows vibrational changes from peptide groups and amino acid side chains which are modified upon Tyr$_D^\bullet$ formation. Proton release at the PS II protein surface upon Tyr$_D^\bullet$ formation is deduced from differential signals at the ν(PO) modes of phosphate.

Photosystem II (PS II)[1] is the membrane protein complex of higher plants, some algae, and cyanobacteria where light energy is converted into a transmenbrane proton gradient and chemical energy with the oxidation of water into dioxygen and the reduction of a plastoquinone, Q_B, into the quinol form Q_BH_2. Two homologous polypeptides, D1 and D2, constitute the binding site of the essential cofactors involved in the light-induced electron and proton transfer reactions [see Michel and Deisenhofer (1988) for a review]. In PS II, absorption of a photon results in the oxidation of

---

[†] R. H. was supported by an EEC fellowship (ERB40016T933365).

* Corresponding author. Fax: 33 1 69 08 87 17. E-mail: berthomieu@dsvidf.cea.fr.

[‡] URA CNRS 2096.

[⊗] Abstract published in *Advance ACS Abstracts,* November 1, 1996.

[1] Abbreviations: PS II (PS I), photosystem II (I); RC, reaction center; D1, D2, polypeptides of PS II; Tyr$_D$, tyrosine D2−160; Tyr$_Z$, tyrosine D1−161; P_{680} (P_{700}), primary chlorophyll electron donor of PS II (PS I); Q_A (Q_B), primary (secondary) electron acceptor plastoquinone; Fe, non-heme iron, cofactor of PS II; (B)Chl, (bacterio)chlorophyll; cresol, *p*-methylphenol; Mes, 2-(*N*-morpholino)ethanesulfonic acid; Tris, tris-(hydroxymethyl)aminomethane; DCMU, 3-(3,4 dichlorophenyl)-1,1-dimethylurea; PMS, phenazine methosulfate; ν, stretching vibration; δ, bending vibration; FTIR, Fourier transform infrared; (cw)EPR, (continuous wave) electron paramagnetic resonance; ESEEM, electron spin echo envelope modulation; ENDOR, electron nuclear double resonance; TRIPLE, electron nuclear nuclear triple resonance; RR, resonance Raman.

S0006-2960(96)01952-6 CCC: $12.00

a chlorophyllic electron donor (P_{680}) and the reduction of a bound plastoquinone (Q_A) which is reoxidized by the exchangeable plastoquinone Q_B. P_{680}^+ is reduced by a redox active tyrosine of the D1 polypeptide, Tyr_Z (D1−161, amino acid numbering from *Synechocystis* sp. PCC 6803; Debus et al., 1988b; Metz et al., 1989). Tyr_Z forms a transient radical that is reduced on the micro- to millisecond time scale by a cluster of four manganese ions acting probably both as the active site and as a charge-accumulating device of the water-splitting enzyme [reviewed in Debus (1992), Diner and Babcock (1996), Rutherford (1989)]. On the homologous polypeptide D2, a symmetry-related tyrosine, Tyr_D (D2−160; Debus et al., 1988a; Vermaas et al., 1988) also forms a neutral radical ($Tyr_D^\bullet$). This radical is stable on the hour time scale in oxygen-evolving PS II (Babcock & Sauer, 1973). $Tyr_D^\bullet$ has still unknown functionality but is involved in slow redox reactions with the Mn cluster under special circumstances [Vass and Styring (1991) and references therein]. The midpoint potential of $Tyr_D^\bullet/Tyr_D$ was determined at 760 mV, while that of $Tyr_Z^\bullet/Tyr_Z$ was estimated at ≈1 V (Boussac & Etienne, 1984; Hoganson & Babcock, 1994). The two tyrosine radicals have been identified spectroscopically by the EPR study of PS II preparations of *Synechocystis* sp. PCC 6803 with specifically labeled tyrosines (Barry & Babcock, 1987; Barry et al., 1990).

To explain the different properties of Tyr_Z and Tyr_D, the structure and interactions of the two tyrosine radicals have been extensively studied by magnetic resonance spectroscopies, including comparison with model compounds. Both radicals give almost identical cw-EPR spectra, characteristic of neutral radicals with similar spin distribution (Diner et al., 1995; Hoganson & Babcock, 1994; Tang et al., 1996). The presence of a hydrogen bond to the $Tyr_D^\bullet$ oxygen was evidenced by electron spin echo envelope modulation (ESEEM; Evelo et al., 1989) and ENDOR (Mino et al., 1993; Rodriguez et al., 1987; Tang et al., 1993) spectroscopies and was also concluded from high-field EPR experiments (Sun et al., 1996). The presence of a hydrogen bond to $Tyr_Z^\bullet$, although more disordered than that to $Tyr_D^\bullet$, has also been recently suggested from ^{2}H-ENDOR, TRIPLE, and high-field EPR experiments on Mn-depleted PS II (Force et al., 1995; Sun et al., 1996; Tang et al., 1996). It has been proposed from ESEEM experiments that the conformation of $Tyr_D^\bullet$ is well defined, while for $Tyr_Z^\bullet$, different orientations of the ring with respect to the tyrosine alkyl chain could exist in Mn- or Ca^{2+}-depleted PS II (Gilchrist et al., 1995; Tommos et al., 1995; Hoganson et al., 1995). Tyr_Z oxidation induces proton release at the PS II membrane surface (Renger & Völker, 1982; Bögershausen & Junge, 1995). To our knowledge, proton release upon $Tyr_D^\bullet$ formation has not been measured so far.

The difference in midpoint potential and in oxidoreduction kinetics of the two tyrosine radicals may rely on local structural asymmetry as discussed from structural models (Ruffle et al., 1992; Svensson, 1995; Svensson et al., 1990). It is proposed that the side chain of His D2−189 is involved in the hydrogen bond to $Tyr_D^\bullet$ (Debus et al., 1988a; Svensson et al., 1990; Tang et al., 1993; Tommos et al., 1993). The implication of the homologous histidine residue on D1 (His D1−190) in the hydrogen bond to $Tyr_Z^\bullet$ is still controversial (Bernard et al., 1995; Diner et al., 1991; Roffey et al., 1994; Tang et al., 1996), and the specific role of the amino acids surrounding Tyr_Z and Tyr_D in tuning the tyrosine properties is not clearly determined.

The nature of the chemical groups involved in the different events of protonation and/or proton transfer upon Tyr_D or Tyr_Z oxidation as well as the conformation and interactions of the tyrosine residues can be addressed by FTIR difference spectroscopy. Vibrational modes of a molecule are very sensitive to its geometry and the dipolar interactions or hydrogen bonds formed with the environment. In contrast to magnetic spectroscopies which selectively address the structure and interactions of the radicals, light-induced FTIR difference spectroscopy is not selective and will provide not only a complementary method for the detailed structural analysis of the tyrosines both in their reduced and radical states but also information with regard to all the cofactors and protein residues perturbed upon tyrosine oxidation [for a review on the method, see Mäntele (1993)]. In particular, (de)protonation or hydrogen bond formation can be directly probed at the IR modes of the amino acids involved. The contributions of the tyrosine radicals in PS II can also be analyzed by comparison with the IR modes of tyrosine and phenoxyl radicals generated by UV irradiation *in vitro* (Berthomieu & Boussac, 1995). The assignment of IR signals to a particular residue can be complicated, however, by complex signal overlaps. Thus, a prerequisite for the vibrational analysis is the optimization of experimental conditions to observe changes due to the oxidation (reduction) of only one redox active intermediate during the FTIR data acquisition.

It is difficult to obtain independently the $Tyr_D^\bullet/Tyr_D$ or $Tyr_Z^\bullet/Tyr_Z$ FTIR spectra and avoid contamination from Q_A^-/Q_A IR signals, since Q_A^- is formed concomitantly to the oxidation of species at the electron donor side of PS II. In certain conditions, a chlorophyll cation (Chl^+) can also be observed under continuous illumination (MacDonald & Barry, 1992; MacDonald et al., 1993). To avoid the photoaccumulation of different charge-separated states under continuous illumination, we have used flash or short illumination of samples in the presence of exogenous electron donors or acceptors. These conditions were optimized to stabilize preferentially only one charged intermediate. Since EPR signals from both the electron acceptor side and donor side are well characterized, and since EPR measurements can be performed in samples in which protein concentration and water content are close to those of IR samples, EPR spectroscopy was used as an independent method to identify the different light-induced intermediates and estimate their lifetimes. We have thus optimized different experimental conditions to record the Q_A^-/Q_A (Berthomieu et al., 1990, 1992a) and $Tyr_D^\bullet/Tyr_D$ (Hienerwadel et al., 1995a,b) FTIR difference spectra free from contributions of other reaction intermediates.

In studies aimed at detecting vibrational modes of Tyr_D and Tyr_Z, light-induced FTIR difference spectra were obtained by steady-state illumination of core PS II samples isolated from spinach (MacDonald & Barry, 1992) or *Synechocystis* sp. PCC 6803 (Bernard et al., 1995; MacDonald et al., 1993). These spectra appear to contain contributions from Q_A^-/Q_A and/or from Chl^+/Chl that are discussed but not fully quantified. Indeed, the difference spectra reported in these studies and attributed to $Tyr_D^\bullet/Tyr_D$ and/or $Tyr_Z^\bullet/Tyr_Z$ transitions (Bernard et al., 1995; MacDonald & Barry, 1992; MacDonald et al., 1993) or to $Chl^+/$

Chl (MacDonald et al., 1995) present similarities to our previously reported spectrum of Q_A^-/Q_A (Berthomieu et al., 1990, 1992a) particularly with respect to large positive contributions at 1477−1480 cm^{-1}. Recently, MacDonald et al. (1995) have proposed that the FTIR difference spectrum that we previously assigned to Q_A^-/Q_A (Berthomieu et al., 1990, 1992a) originates mainly from Chl^+/Chl. In particular, whereas we (Berthomieu et al., 1990, 1992a) and others (Araga et al., 1993; Noguchi et al., 1992) have assigned the largest positive band in our spectrum (at 1478 cm^{-1}) to the Q_A^- state, MacDonald et al. (1995) assign this band to Chl^+. Unfortunately, MacDonald et al. (1995) did not monitor the contributions of Q_A^- to their spectra.

We describe herein the details of the EPR control experiments that show that our Q_A^-/Q_A FTIR difference spectrum contains no detectable contributions from either Chl^+/Chl or $Tyr_D^•/Tyr_D$. In addition, we present a comparison between a $Tyr_D^•/Tyr_D$ FTIR spectrum free from contributions of other reaction intermediates and the radical-*minus*-non-radical FTIR difference spectra obtained by UV irradiation at 10 K of cresol (*p*-methylphenol), a model compound of the tyrosine side chain.

MATERIALS AND METHODS

PS II-enriched membranes were prepared from spinach, and Mn depletion was performed by Tris treatment as previously described (Hienerwadel & Berthomieu, 1995). For the study of Tyr_D, Tris-treated PS II-enriched membranes were incubated for 1 h at 4 °C in N_2-degassed buffer A (50 mM phosphate, 10 mM NaCl, 5 mM $MgCl_2$) at pH 6 in the presence of 100 mM formate followed by centrifugation (100000*g*, 15 min) and two successive washing steps in buffer A at pH 6 in the presence of 50 mM formate. The membranes were then pelleted. H/D exchange was performed by incubation of the sample at 8 °C overnight in a phosphate buffer in D_2O at pD 8 in the presence of 100 mM formate followed by centrifugation and two successive washing steps in buffer A in D_2O at pD 6 in the presence of 50 mM formate.

The FTIR sample consisted of a fraction of the membrane pellets deposited between two CaF_2 windows (chlorophyll concentration larger than 15 mg/mL). For the Tyr_D experiments, 5 μL of a 0.5 M ferricyanide solution was first dried onto one of the windows. The membrane pellet was then deposited and squeezed between the two windows. The $Tyr_D^•/Tyr_D$ FTIR difference spectrum was obtained by taking 80 scans (corresponding to a recording time of ≈14 s) before and 2 s after illumination of the sample. The same FTIR difference spectra were obtained with single laser flash or a 1 s illumination with a 680 nm laser diode, the latter illumination giving larger signals. The acquisitions were cycled during about 15 h, with dark periods of ≈12 min between successive illuminations. No alteration of the FTIR difference signals was observed during the acquisition duration. Spectra obtained with 6−10 samples were averaged. The measurements were performed at 4 °C for samples in H_2O and at 6 °C for samples in D_2O.

For the study of Q_A, PS II-enriched membranes were resuspended in Mes/NaOH buffer (50 mM Mes, 10 mM NaCl) at pH 6.4 in the presence of 10 mM NH_2OH, 0.1 mM DCMU, and 2 mM PMS as described (Berthomieu et al., 1992a). ^{15}N-Labeling of spinach PS II-enriched membranes was obtained as described (Zimmermann et al., 1993). From ESEEM experiments, the extent of ^{15}N-labeling was estimated to be larger than 85% in these membranes (Deligiannakis et al., 1995). The Q_A^-/Q_A FTIR difference spectra were obtained by taking 64 scans (11 s duration) before and after illumination by a saturating flash from a Nd-Yag laser. Spectra were recorded at 10 °C.

The cresol radical was obtained by UV irradiation at 10 K as described for phenol (Berthomieu & Boussac, 1995). Cresol (0.2 M) was dissolved in borate buffer (0.2 M) at pH 8 in H_2O or at pD 8 in D_2O. The FTIR difference spectra were obtained by taking 768 scans before and after illumination (Berthomieu & Boussac, 1995). Spectra obtained with 9−11 samples were averaged.

FTIR spectra were recorded on a Bruker IFS 88 SX spectrometer equipped with a thermostated sample wheel and a N_2- or He-cooled cryostat. Illumination of the sample was either performed by the broad band emission of sulforhodamine 101 pumped by the 15 ns pulse of a frequency-doubled Nd-Yag laser (Quantel YG 780-50) or by a 1 s illumination with a 680 nm laser diode of 20 mW output power (LaserMax Inc.). Spectra were recorded with 4 cm^{-1} resolution.

The EPR sample consisted of a fraction of the membrane pellet (same as used for FTIR) deposited on a mylar strip in an EPR tube closed under helium atmosphere. For experiments performed at 4 °C, the samples were illuminated directly in the EPR cavity. Illumination at 200 K was performed in a glass Dewar filled with CO_2−ethanol mixture. Continuous or short illumination was performed with a 800 W tungsten lamp through water, red, and Calflex filters. Flash illumination was performed by a Nd-Yag laser (Quantel; 300 mJ at 532 nm, 15 ns pulse duration).

cw-EPR spectra were recorded at 4 °C or at helium temperature on a Bruker ER 200D X-band spectrometer equipped with an Oxford Instruments cryostat or a Bruker B-VT1000 N_2 gas flow system, a HP5350B microwave frequency counter, and a Bruker ER 35 NMR gaussmeter for the detection of the **g** values.

RESULTS

Experimental conditions have been developed to obtain independently the light-induced FTIR difference spectra corresponding either to Tyr_D oxidation or to the primary quinone Q_A reduction. The formation and decay of $Tyr_D^•$ and Q_A^- were monitored with EPR spectroscopy on samples which consisted of a fraction of the same pellet treated with the same procedure as used for the FTIR measurements and which were deposited on mylar strips in the EPR tubes.

Recording the $Tyr_D^•/Tyr_D$ FTIR difference spectrum requires that (i) Tyr_D is reduced in a large fraction of PS II centers in the dark-adapted state, (ii) Tyr_D becomes photooxidized with high yield, and (iii) $Tyr_D^•$ decays after illumination with kinetics suitable both for the acquisition of the FTIR spectrum and for the cycling of the light-induced experiment, i.e., in the minute time range. These measurements also necessitate that the semiquinone Q_A^- formed by the light-induced charge separation is reoxidized rapidly and completely before the acquisition of the FTIR spectrum is started.

In Mn-depleted PS II-enriched membranes, $Tyr_D^•$ becomes reduced in the minute time range at high pH or in the presence of reductants [see, for example, Boussac and Etienne (1982a,b), Vass et al. (1990)]. To obtain the IR changes induced by Tyr$_D^\bullet$ formation, we have investigated Tris-washed PS II membranes at pH 6 in the presence of ferricyanide and ferrocyanide. Ferricyanide was added to the sample as efficient exogenous electron acceptor from Q$_A^-$. It was observed in the IR absorption of the sample at 2150−2050 cm^{-1} that 5−10% of the ferricyanide was converted into ferrocyanide in the dark-adapted sample before starting the FTIR experiment (not shown). This fraction of ferrocyanide is probably at the origin of Tyr$_D^\bullet$ reduction. Ferricyanide and ferrocyanide signals are easy to follow since they absorb in a specific IR frequency range, which is distinct from the absorption region of interest for the study of cofactors and protein modes. Ferricyanide can however oxidize the non-heme iron located between the quinones Q$_A$ and Q$_B$ (Ikegami & Katoh, 1973; Petrouleas & Diner, 1986), which in turn can be rapidly reduced by Q$_A^-$. The iron photoreduction is stable for several seconds and gives a characteristic FTIR difference spectrum (Hienerwadel et al., 1993; Hienerwadel & Berthomieu, 1995; Noguchi & Inoue, 1995a). To avoid this reaction, formate was added to the sample. Bicarbonate displacement by formate in the non-heme iron environment results in an increase of the midpoint potential of the iron above 500 mV at pH 6 (Deligiannakis et al., 1994) such that the non-heme iron can no longer be oxidized by ferricyanide. It was observed that addition of formate allows a fast reoxidation of Q$_A^-$ by ferricyanide in the FTIR sample conditions. The presence of phosphate in the buffer also seems to accelerate the reduction of Tyr$_D^\bullet$ in the dark within 12 min at pH 6 (see below). This was essential for cycling the light-induced FTIR difference spectra in order to obtain highly resolved Tyr$_D^\bullet$/Tyr$_D$ spectra at 4 °C without contributions from the electron acceptor side of PS II.

EPR Controls for the FTIR Study of Tyr$_D$ Oxidation. Figure 1A shows the EPR spectra in the $\mathbf{g} = 2$ region recorded at 4 °C with Tris-washed PS II-enriched membranes isolated from spinach and resuspended at pH 6 in the presence of phosphate, formate, and ferricyanide. Spectrum a in Figure 1A shows the Tyr$^\bullet$ EPR signal recorded under continuous illumination of the sample directly in the EPR cavity. Spectrum a is about 1.5 times larger than spectrum b, which is recorded just after a 1 s illumination of the sample directly in the EPR cavity (acquisition time of ≈20 s). Contributions from both Tyr$_D^\bullet$ and Tyr$_Z^\bullet$ are expected in spectrum a recorded under illumination. Only contributions from Tyr$_D^\bullet$ are expected in spectrum b, since Tyr$_Z^\bullet$ decays in the millisecond time range after illumination in Tris-washed PS II membranes in the presence of ferricyanide and ferrocyanide (Dekker et al., 1984). In Mn-depleted PS II, Tyr$_Z^\bullet$ reduction occurs in the millisecond to second time range either by recombination with Q$_A^-$ or Q$_B^-$ or by the action of exogenous reductants [reviewed in Hoganson and Babcock (1994)]. Spectrum c in Figure 1A was recorded after a dark period of 8 min following the 1 s illumination. Almost no Tyr$^\bullet$ EPR signal is observed in this spectrum. The Tyr$^\bullet$ EPR signal has completely decayed within 12 min (spectrum d). The decay of the photoinduced Tyr$^\bullet$ EPR signal is more precisely described by the decay kinetic recorded following flash light illumination (Figure 1B) at 4 °C and at the field position indicated by the arrow in Figure 1A (3340 G). The dark-adapted sample was illuminated by three successive laser flashes spaced by 1.6 s. On each flash, the decay of the signal is biphasic, with a fast component ($t_{1/2}$ < 1 s) and a slow component with a half-time of ≈70 s, as determined after the third flash. The two components are formed in comparable amount on the first flash. The presence of two components with different reduction kinetics, formed in equivalent amounts on the first flash, and the total disappearance of the Tyr$^\bullet$ EPR signal within 12 min (Figure 1A) argue that the fast disappearing component corresponds to Tyr$_Z^\bullet$ while the slow decaying species corresponds to Tyr$_D^\bullet$. Similar decay kinetics were obtained after a 1 s continuous illumination (not shown). This procedure matches that used for FTIR spectroscopy. Spectra c and d reveal the presence of a small narrow signal at $\mathbf{g} \approx 2$ in a small fraction of PS II centers. The origin of this signal is at present unknown. By contrast with the Tyr$^\bullet$ EPR signal, this signal is stable. The inset of Figure 1B shows the difference spectrum obtained by subtracting spectrum b from spectrum c. The shape of this difference signal matches perfectly the one expected for Tyr$_D^\bullet$ [Hoganson and Babcock

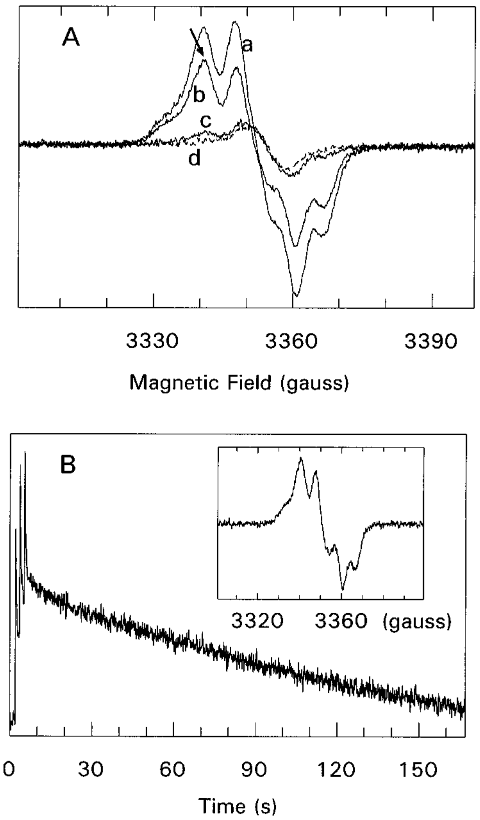

FIGURE 1: (A) EPR spectra recorded with Tris-washed PS II-enriched membranes from spinach at pH 6, in the presence of phosphate, formate, and ferricyanide. The membrane pellet is deposited on mylar strips in the EPR tube, and the spectra are recorded at 4 °C. Spectrum a is recorded under continuous illumination, spectrum b is recorded directly after a 1 s illumination, spectrum c is recorded 8 min after the 1 s illumination, and spectrum d (dashed line) is recorded 12 min after the 1 s illumination. Experimental conditions: microwave power, 1.6 mW; modulation amplitude, 2.65 G; modulation frequency, 100 kHz; microwave frequency, 9.42 GHz. (B) Decay kinetic of the tyrosine radical EPR signal recorded at 3340 G (at the position of the arrow in part A) after illumination by three laser flashes spaced by 1.6 s. Average of 12 kinetic traces, recorded every 200 s at 4 °C. Experimental conditions: microwave power, 20 mW; modulation amplitude, 6.6 G; modulation frequency, 100 kHz; microwave frequency, 9.4 GHz; time constant, 40 ms. Inset: EPR difference spectrum calculated from spectrum b minus spectrum c of part A.

(1994) and references therein]. Thus it is concluded that only Tyr$_\mathrm{D}^\bullet$ is formed after 1 s illumination.

With repetitive flashes as in Figure 1B or with a short continuous illumination, Tyr$_\mathrm{D}^\bullet$ can be accumulated in a large fraction of PS II centers. The fraction of Tyr$_\mathrm{D}^\bullet$ that can be generated at 4 °C has been estimated as follows. The sample illuminated at 4 °C for 1 s was rapidly frozen to 77 K, and the Tyr$_\mathrm{D}^\bullet$ EPR signal recorded at 15 K was integrated two times. The sample was then rewarmed to 200 K and further illuminated. It was observed in a parallel experiment on Tris-washed PS II-enriched membranes at pH 6.5 that illumination at 200 K will form Chl$^+$ in PS II centers in which Tyr$_\mathrm{D}^\bullet$ is already present in the dark or predominantly Tyr$_\mathrm{D}^\bullet$ in centers in which it was reduced [data not shown, see Buser et al. (1992)]. Therefore, after the 200 K illumination Tyr$_\mathrm{D}^\bullet$ is expected in the majority of the PS II centers. In the EPR spectrum recorded at 15 K, the narrow Chl$^+$ EPR signal (ΔH = 10 G, $\mathbf{g}$ = 2.0025) appears superimposed to the Tyr$_\mathrm{D}^\bullet$ EPR signal (ΔH = 24 G, $\mathbf{g}$ = 2.0044). The amount of Tyr$_\mathrm{D}^\bullet$ formed after illumination at 200 K was estimated after subtraction of this Chl$^+$ narrow EPR signal from the EPR spectrum recorded at $\mathbf{g} \approx 2$. To obtain a pure Chl$^+$ EPR signal, the Tyr$_\mathrm{D}^\bullet$ contributions from the EPR spectrum recorded at 15 K after the 200 K illumination were canceled by interactive subtraction of the Tyr$_\mathrm{D}^\bullet$ EPR spectrum obtained after illumination at 4 °C. A similar protocol has been used to identify the different radicals induced by low-temperature illumination (Buser et al., 1992). The Tyr$_\mathrm{D}^\bullet$ EPR signal formed upon the 1 s illumination at 4 °C was estimated to about 90% of that recorded after the 200 K illumination (on the basis of the integrated signal areas). The EPR data described in Figure 1 indicate that Tyr$_\mathrm{D}^\bullet$ is formed with high yield in the conditions used for FTIR spectroscopy. It is also shown that no contribution from Tyr$_\mathrm{Z}^\bullet$ is expected 2 s after illumination. The acquisition of the FTIR spectrum for the illuminated sample is therefore started 2 s after the end of the illumination (see below) to avoid contribution from Tyr$_\mathrm{Z}^\bullet$/Tyr$_\mathrm{Z}$ signals.

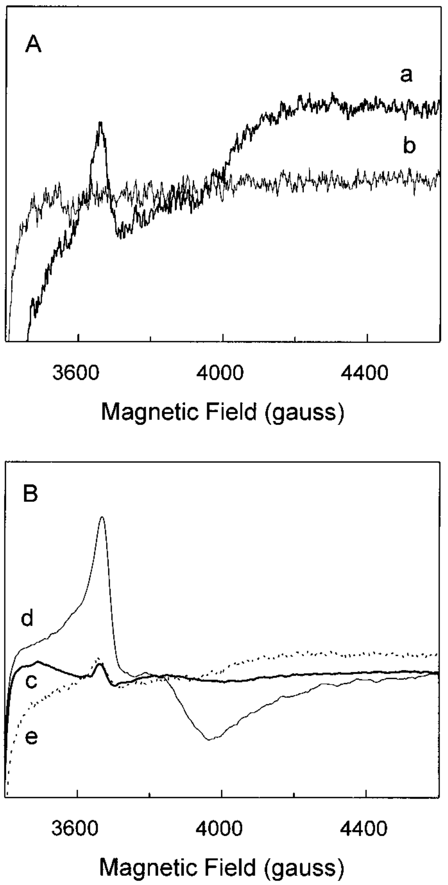

FIGURE 2: $\mathrm{Q_A}^-{-}\mathrm{Fe}^{2+}$ EPR signals recorded at 4.6 K on the same PS II sample as described in Figure 1. (A) Spectrum a (thick line) was generated by a 1 min illumination at 200 K. Spectrum b (thin line) was generated by a 1 s illumination at 4 °C followed by freezing to 77 K. Experimental conditions: microwave power, 32 mW; amplitude modulation, 32 G; modulation frequency, 100 kHz; microwave frequency, 9.4 GHz. (B) $\mathrm{Q_A}^-{-}\mathrm{Fe}^{2+}$ EPR spectra generated by 1 min illumination at 200 K in Tris-washed PS II samples in Mes buffer at pH 6: spectrum c (thick line), sample with 0.5 mM ferricyanide; spectrum d (thin line), sample in the presence of phosphate and 50 mM formate; spectrum e (dashed line), sample in the presence of phosphate, formate, and ferricyanide. The samples consist of membrane pellets deposited on a mylar strip. The signals are calibrated to the same PS II center concentration, as estimated by the size of the Tyr$_\mathrm{D}^\bullet$-stable EPR signal obtained after a 200 K illumination. Experimental conditions: microwave power, 32 mW; amplitude modulation, 32 G; modulation frequency, 100 kHz; microwave frequency, 9.4 GHz.

Upon sample illumination, the primary electron acceptor Q$_\mathrm{A}$ is reduced simultaneously to Tyr$_\mathrm{D}$ and Tyr$_\mathrm{Z}$ oxidation. The semiquinone−iron complex ($\mathrm{Q_A}^-{-}\mathrm{Fe}^{2+}$) gives rise to an EPR signal detected at $\mathbf{g} \approx 1.9{-}1.82$ and 4.6 K in Tris-washed PS II samples (Rutherford & Zimmermann, 1984). Illumination at 200 K is expected to form $\mathrm{Q_A}^-$ in almost all PS II centers (Rutherford & Zimmermann, 1984). Therefore, the maximum amount of $\mathrm{Q_A}^-$ present in the samples was determined by the size of the semiquinone−iron EPR signal obtained by illumination at 200 K. This signal is shown in spectrum a of Figure 2A. The $\mathrm{Q_A}^-{-}\mathrm{Fe}^{2+}$ EPR signal at 4.6 K is clearly observed at $\mathbf{g}$ = 1.82 (≈3700 G) despite the intense signal of ferricyanide which is responsible for a slope of the base line in this magnetic field region. Spectrum b shows the EPR signal at 4.6 K obtained after illumination at 4 °C followed by fast freezing of the sample. This procedure is expected to trap the $\mathrm{Q_A}^-$ state which has not been reoxidized within the approximate 2 s required to freeze the EPR sample. The absence of a detectable $\mathrm{Q_A}^-{-}\mathrm{Fe}^{2+}$ EPR signal in spectrum b (thin line) demonstrates that $\mathrm{Q_A}^-$ is reoxidized by ferricyanide within about 2 s for almost all (if not all) PS II centers. In the presence of formate, it is known that the $\mathrm{Fe}^{2+}{-}\mathrm{Q_A}^-$ EPR signal is considerably enhanced (Vermaas & Rutherford, 1984) which seems not to be the case in spectrum a (Figure 2A). To address this question, the $\mathrm{Q_A}^-{-}\mathrm{Fe}^{2+}$ EPR spectra obtained by illumination at 200 K have been compared for Tris-washed PS II membranes resuspended in Mes buffer at pH 6 in the presence of (i) 0.5 mM ferricyanide (spectrum c, Figure 2B), (ii) phosphate and formate (spectrum d, Figure 2B), and (iii) phosphate, formate, and ferricyanide (spectrum e, Figure 2B). The $\mathrm{Q_A}^-{-}\mathrm{Fe}^{2+}$ EPR spectra displayed in Figure 2B have been scaled to the same concentration of PS II centers, estimated by the size of the Tyr$_\mathrm{D}^\bullet$ EPR signal (measured as described above). The $\mathrm{Q_A}^-{-}\mathrm{Fe}^{2+}$ EPR signal recorded in the sample with formate and without ferricyanide (Figure 2B, spectrum d) is largely enhanced, as compared to the signal obtained in the Tris-washed PS II sample (spectrum c). The $\mathrm{Q_A}^-{-}\mathrm{Fe}^{2+}$ EPR signal observed in the sample with formate and ferricyanide (spectrum e) is comparable in size to the $\mathrm{Q_A}^-{-}\mathrm{Fe}^{2+}$ EPR signal obtained with the Tris-washed PS II sample (spectrum c). This indicates that the $\mathrm{Q_A}^-{-}\mathrm{Fe}^{2+}$ EPR signal obtained by illumination at 200 K of the

PS II sample in the presence of formate, phosphate, and ferricyanide indeed corresponds to Q_A^- formation in almost all PS II centers but that addition of ferricyanide suppresses the enhancement effect on the $Q_A^-{-}Fe^{2+}$ EPR signal due to formate binding. In samples with bound formate, the magnetic coupling between the semiquinone and the iron is probably modified by binding of ferricyanide in a specific site around Q_A. The reoxidation of Q_A^- by ferricyanide in these samples is fast, as demonstrated by the absence of a detectable $Q_A^-{-}Fe^{2+}$ EPR signal 2 s after illumination at 4 °C. No light-induced EPR signal was observed in the field region of the Fe^{3+} EPR signal (not shown).

In conclusion, the EPR measurements performed on Tris-washed PS II membranes in the presence of phosphate, formate, and ferricyanide show that only IR changes due to Tyr_D oxidation and ferricyanide reduction will contribute to the illuminated-*minus*-dark-adapted FTIR difference spectra if the acquisition of the illuminated spectrum is started 2 s after illumination (1 s) at 4 °C. In addition, the decay of $Tyr_D^{\bullet}$ within 12 min presents a major advantage for the cycling of the light-induced FTIR experiments. Finally, the shape of the light-induced $Tyr_D^{\bullet}$ EPR signal (Figure 1B, inset) was identical in these conditions as with Tris-washed PS II-enriched membranes at pH 6, indicating that these experimental conditions induce no change of the $Tyr_D^{\bullet}$ structure.

EPR Controls for the FTIR Study of Q_A Reduction. Previously, we have reported FTIR difference spectra assigned to IR changes induced by the photoreduction of the plastoquinone Q_A (Berthomieu et al., 1990, 1992a). The Q_A^-/Q_A FTIR difference spectra were obtained at 10 °C using PS II-enriched membranes isolated from spinach and incubated in the presence of hydroxylamine (NH_2OH) as fast electron donor and DCMU to block electron transfer from Q_A^- to Q_B. In Berthomieu et al. (1992a), phenazine methosulfate (PMS) was added as electron acceptor from Q_A^- to cycle the light-induced experiments. Recently, a similar FTIR difference spectrum was obtained by MacDonald et al. (1995) with different experimental conditions and interpreted as dominated by Chl^+/Chl contributions. We present in Figure 3 the EPR controls performed in the experimental conditions that were previously developed to record the Q_A^-/Q_A FTIR spectrum (Berthomieu et al., 1990, 1992a). The spectral regions of both the $Q_A^-{-}Fe^{2+}$ and the Chl^+ or $Tyr^{\bullet}$ EPR signals have been investigated.

Figure 3A shows the $Q_A^-{-}Fe^{2+}$ EPR signals recorded at 4.6 K in a Tris-washed PS II sample in the presence of NH_2-OH, PMS, and DCMU. No signal is observed in spectrum a (thin line) which is obtained for the sample dark-adapted for 2 min at 10 °C before freezing. Spectrum b (thick line) is recorded on the sample which was illuminated for 1 s at 10 °C and then quickly frozen to 77 K. This procedure will trap the photoreduced Q_A^- still present in the sample after the time required to freeze the sample (≈2 s). Spectrum c (dashed line) is recorded after a further illumination (1 min) of the sample at 200 K. In these conditions, we expect an almost complete reduction of Q_A, since no electron transfer from Q_A^- to PMS occurs at 200 K (see below). Thus, the $Q_A^-{-}Fe^{2+}$ EPR signal in spectrum c represents the maximum amount of Q_A^- that can be photoreduced in the sample. The amplitude of spectrum b corresponds to ≈40% of the amplitude of spectrum c. Therefore, ≈2 s after illumination at 10 °C, Q_A^- can be trapped in about 40% of the PS II RCs. These results confirm that Q_A^- is actually formed in a significant fraction of PS II RCs in the sample conditions used for the FTIR measurements.

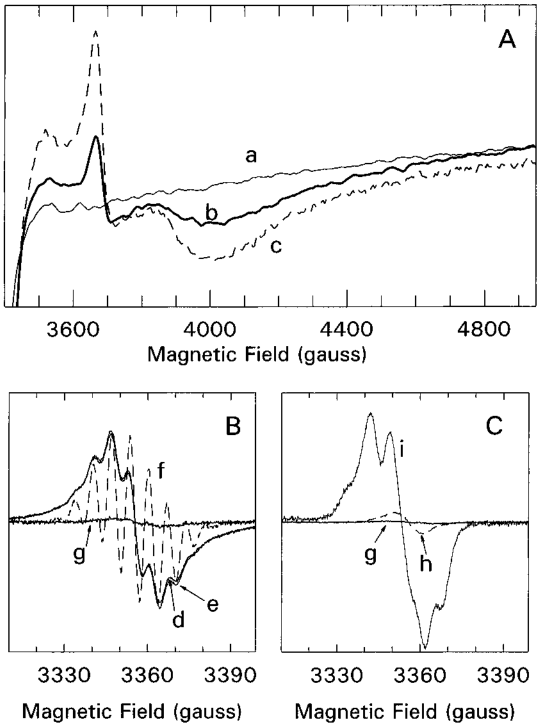

FIGURE 3: Tris-treated PS II membranes at pH 6.4 in the presence of 10 mM hydroxylamine, 2 mM PMS, and 0.5 mM DCMU. Membrane pellets are deposited on a mylar strip. (A) $Q_A^-{-}Fe^{2+}$ EPR signals recorded at 4.6 K: spectrum a (thin line), sample dark-adapted for 2 min at 10 °C before freezing; spectrum b (thick line), sample illuminated for 2 s at 10 °C and frozen at 77 K and then to 4.6 K; spectrum c (dashed line), sample after a further illumination for 1 min at 200 K. Experimental conditions: microwave power, 32 mW; amplitude modulation, 32 G; modulation frequency, 100 kHz; microwave frequency, 9.4 GHz. (B) EPR spectra recorded at $\mathbf{g} \approx 2$ at 10 °C in the conditions used for FTIR experiments. Spectra d and e (12 s sweep time) are recorded before and immediately after a 1 s illumination directly in the EPR spectrometer cavity. Spectra d and e are the result of the average of 16 subsequent measurements with 1 min delay between consecutive illuminations. Spectrum f (dashed line) shows the PMS^- EPR signal recorded in the resuspension buffer in the absence of the PS II membranes. The scale of this spectrum was adjusted to that of spectrum d. Spectrum g is calculated by the difference spectrum e minus spectrum d. Experimental conditions: microwave power, 8 mW; modulation amplitude, 2.6 G; modulation frequency, 100 kHz; microwave frequency, 9.4 GHz. (C) Spectrum g (same as in part B) compared to the EPR spectrum of the dark-stable $Tyr^{\bullet}$ EPR signal (spectrum i, thin line) measured on a Tris-washed PS II sample with the same RC concentration and compared to Chl^+ EPR spectrum h (dashed line), scaled to correspond to 5% of the number of spins of spectrum i (calculated by double integration of the signals). Experimental conditions were as described for part B.

In the same sample, the electron donor side has been monitored by EPR measurements around $\mathbf{g} = 2$ and at 10 °C. The EPR spectra were recorded before (dark-adapted sample) and immediately after (illuminated sample) a 1 s continuous illumination directly in the EPR cavity. The sweep time for each spectrum is 12 s, and the spectra result from the average of 16 traces with a 1 min delay between two subsequent illuminations. The acquisition duration and the dark period between consecutive illuminations are almost identical with those used to record the FTIR difference spectra. The EPR spectra d and e in Figure 3B correspond to the dark-adapted and illuminated samples, respectively. These spectra are almost superimposable. Spectrum f is recorded in the PS II resuspension buffer but in the absence of PS II sample. This spectrum corresponds to the EPR signal of PMS^-, probably due to partial PMS reduction by NH_2OH in the buffer. The hyperfine coupling and **g** value (**g** = 2.0031) of spectra d and e of the dark-adapted and illuminated PS II samples are very similar to those observed in spectrum f (dashed line). Therefore, these EPR signals correspond to spectra of the PMS^- radical. The slight difference in shape between spectra d and e and spectrum f is probably explained by the fact that PMS is immobilized in the PS II pellet and freely mobile in solution. The EPR difference spectrum illuminated-*minus*-dark-adapted calculated from spectra d and e is displayed in spectrum g (Figure 3B). This spectrum is almost a base line. Once expanded, it is similar in shape to spectra d and e (not shown). Figure 3C compares the size of the EPR difference spectrum g (illuminated-*minus*-dark-adapted) with that of the EPR spectrum of stable $Tyr_D^•$ expected for a Tris-washed sample at pH 6 with the same RC concentration but not incubated with NH_2OH (spectrum i). The RC concentration in the two samples has been evaluated using the size of the $Q_A^-{-}Fe^{2+}$ EPR signal obtained by a 200 K illumination in each sample. It was verified in a parallel experiment performed with liquid EPR samples with the same concentration of total chlorophyll (4 mg/mL) that the size of the $Q_A^-{-}Fe^{2+}$ EPR spectrum obtained by illumination at 200 K was comparable for the Tris-washed PS II sample at pH 6 and for the PS II sample in the presence of NH_2OH, PMS, and DCMU. From spectra i and g in Figure 3C, we conclude that the concentration of PMS^- increases only marginally upon illumination. Spectrum h (dashed line) in Figure 3C represents a Chl^+ EPR signal (ΔH = 10 G, **g** = 2.0025) of PS II obtained independently, the size of which has been adjusted to correspond to 5% of the $Tyr_D^•$ EPR signal displayed in spectrum i (spectra h and i are compared on the basis of the integrated signal area). This signal would be observed if illumination would form Chl^+ in 5% of the PS II centers in the sample. Comparison of spectra g and h in Figure 3C confirms that neither $Tyr^•$ nor Chl^+ EPR signals are detected in the sample upon 1 s illumination at 10 °C.

In conclusion, Figure 3 shows that addition of PMS, NH_2OH, and DCMU prevents the formation of any detectable radical on the donor side of PS II upon illumination at 10 °C. These experimental conditions lead to the formation of Q_A^- with a stability suitable for detection by FTIR difference spectroscopy.

FTIR Difference Spectroscopy. The FTIR difference spectrum recorded at 10 °C on PS II-enriched membranes at pH 6.4 in the presence of NH_2OH, PMS, and DCMU is shown in Figure 4A. It was obtained from two IR absorption spectra recorded during 11 s before and after illumination of the sample by a saturating flash. Spectra from several light cycles were averaged. The dark period between two consecutive illuminations was 1 min. As discussed above, EPR controls demonstrate that only contributions due to Q_A reduction are expected in this FTIR spectrum which is thus denoted Q_A^-/Q_A. In particular, it has been shown that no Chl^+ formation was detected in these conditions. We demonstrated previously that there are no common features between this spectrum and a PMS^-/PMS FTIR spectrum generated by electrochemistry (Berthomieu et al., 1992a). In particular, the largest positive band of the PMS^-/PMS spectrum at 1487 cm^{-1} is not observed in Figure 4A. The main absorption band of NH_2OH in H_2O at 1532 cm^{-1} is largely downshifted in D_2O (not shown). The strong similarity in this frequency region between Q_A^-/Q_A spectra obtained in H_2O (Figure 4A) and in D_2O (Berthomieu, 1991; Berthomieu et al., 1990) reveals that NH_2OH does not contribute to the FTIR difference spectrum. In the Q_A^-/Q_A FTIR difference spectrum, the negative and positive signals correspond to the Q_A and Q_A^- states, respectively. The characteristic features of the Q_A^-/Q_A FTIR spectrum are positive signals at 1478, 1417, and 1365 cm^{-1}, a differential signal at 1724/1719 cm^{-1}, and several bands in the 1680−1600 and 1560−1520 cm^{-1} regions, negative bands at 1682, 1672, 1657, 1644, 1630, 1560, and 1542 cm^{-1} and positive signals at 1660, 1625, 1550, and 1530 cm^{-1}.

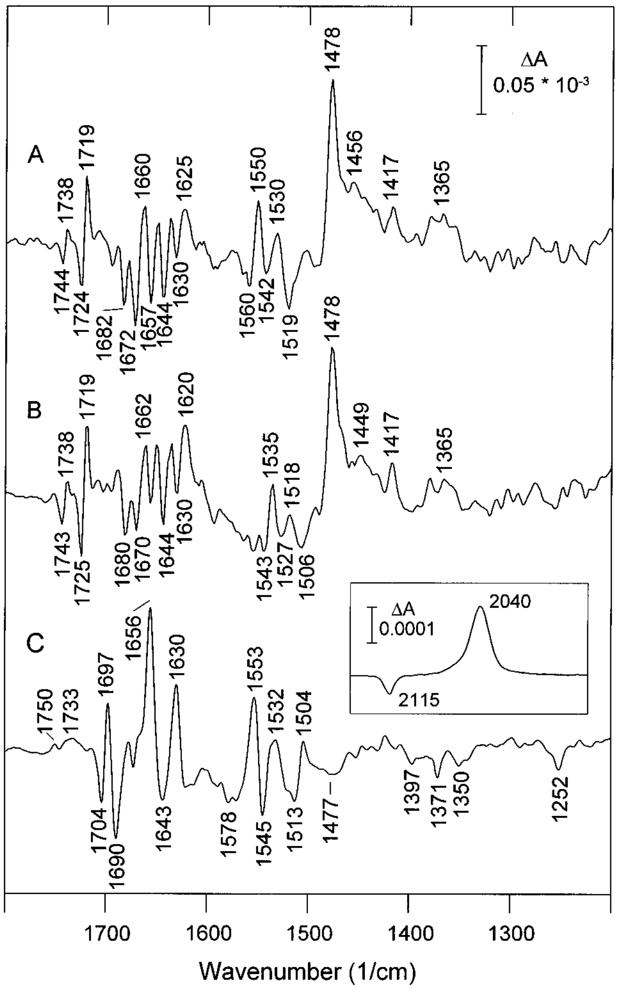

FIGURE 4: FTIR difference spectra of the Tyr_D radical formation and Q_A reduction in Tris-washed PS II membranes. (A) Q_A^-/Q_A spectrum obtained on Tris-washed PS II membranes in Mes buffer (pH 6.4) in the presence of 10 mM NH_2OH, 2 mM PMS, and 0.1 mM DCMU; 24 000 scans, 10 °C, 4 cm^{-1} resolution. (B) Q_A^-/Q_A spectrum obtained on ^{15}N-labeled PS II membranes in the same conditions as above; 8000 scans, 4 cm^{-1} resolution. (C) $Tyr_D^•/Tyr_D$ spectrum obtained in phosphate buffer (pH 6) in the presence of 50 mM formate and ferricyanide; measuring conditions as in Figure 1B, 374 400 scans, 4 °C. Inset 2150−1900 cm^{-1} region of the $Tyr_D^•/Tyr_D$ spectrum.

Figure 4B shows the Q_A^-/Q_A spectrum recorded on ^{15}N-labeled PS II membranes from spinach. All of the differential signals observed at 1560/1550/1542 cm^{-1} in Figure 4A are downshifted to 1543/1535/1527 cm^{-1} in Figure 4B for the ^{15}N-labeled PS II sample. This downshift by about 15 cm^{-1} is characteristic for amide II [ν(CN) + δ(NH)] modes of the peptide backbone (Susi, 1969). The downshift of the totality of these signals upon ^{15}N-labeling indicates that a very high percentage of the amide nitrogens are ^{15}N-labeled in the preparation. This is consistent with the observation that ^{15}N-labeling affects the whole amide II absorption band observed at 1549 and 1536 cm^{-1} in the FTIR absorption spectra of the ^{14}N- and ^{15}N-labeled samples, respectively (Berthomieu, 1991). ESEEM spectroscopic measurements performed on the same PS II membranes confirmed that the efficiency of the ^{15}N-labeling was above 85% (Deligianakis et al., 1995). The FTIR spectra were recorded with 4 cm^{-1} resolution, and the frequencies are given with $\pm$1 cm^{-1} accuracy. Additional effects of ^{15}N-labeling in the Q_A^-/Q_A spectrum consist in the disappearance of the positive band at 1456 cm^{-1} and in the downshift by 2 cm^{-1} of two negative bands at 1682 and 1672 cm^{-1}. A 2 cm^{-1} downshift is much smaller than that expected for ν-(CN) modes of amino acid side chains but is in agreement with the contribution of peptide carbonyl stretching modes (amide I mode) at 1682 and 1672 cm^{-1}. In contrast to these modified modes, some signals are unaltered in the Q_A^-/Q_A spectrum obtained on ^{15}N-labeled PS II. This is the case for two negative bands at 1644 and 1630 cm^{-1} and for the positive bands at 1478 and 1417 cm^{-1}. The frequency difference of 1 cm^{-1} observed in Figure 4A,B at 1743 and 1725 cm^{-1} cannot be considered as significant yet. Since they are not affected by ^{15}N-labeling, the signals at 1644 and 1630 cm^{-1} are possible candidates for the ν(C=O) vibration of the neutral plastoquinone Q_A, while the positive signal at 1478 cm^{-1} has been tentatively assigned to the ν(C$\overset{\cdots}{-}$O) vibration of the semiquinone anion Q_A^- (Berthomieu et al., 1992a).

The FTIR difference spectrum recorded on Tris-washed PS II-enriched membranes at pH 6 in the presence of formate and ferricyanide is shown in Figure 4C. This illuminated-*minus*-dark-adapted spectrum corresponds to the difference between the IR absorption spectra of the sample recorded before and 2 s after a 1 s illumination at 4 °C. The recording of each absorption spectrum takes ≈14 s. The EPR controls demonstrate that only contributions due to Tyr_D oxidation and ferricyanide reduction are expected in this FTIR spectrum, which is therefore denoted $Tyr_D^•/Tyr_D$. The inset shows the 2150−1900 cm^{-1} frequency region of the spectrum, where the ferricyanide and ferrocyanide ν(C≡N) stretching modes contribute at 2115 and 2040 cm^{-1}, respectively. The negative band at 2115 cm^{-1} and the positive one at 2040 cm^{-1} indicate that ferricyanide was reduced after sample illumination and confirm its role as electron acceptor. In the 1800−1000 cm^{-1} range, changes of the order of 10^{-4}–10^{-5} absorption units are observed, which correspond to a small number of perturbations of Tyr_D and neighboring or more distant amino acids or cofactors affected by protonation and/or charge accumulation that occur upon Tyr_D oxidation. The absence of contributions from the electron acceptor side in the $Tyr_D^•/Tyr_D$ spectrum is further demonstrated by comparison of the $Tyr_D^•/Tyr_D$ spectrum (Figure 4C) with the Q_A^-/Q_A spectrum (Figure 4A). The characteristic features of the Q_A^-/Q_A FTIR spectrum are absent in Figure 4C. This is particularly well illustrated by the absence in Figure 4C of the differential signal at 1724/1719 cm^{-1} and the large positive signal at 1478 cm^{-1}. Together with the EPR controls (Figures 1−3), the spectra displayed in Figure 4 demonstrate that experimental conditions have been achieved where Q_A or Tyr_D can be studied independently by FTIR difference spectroscopy.

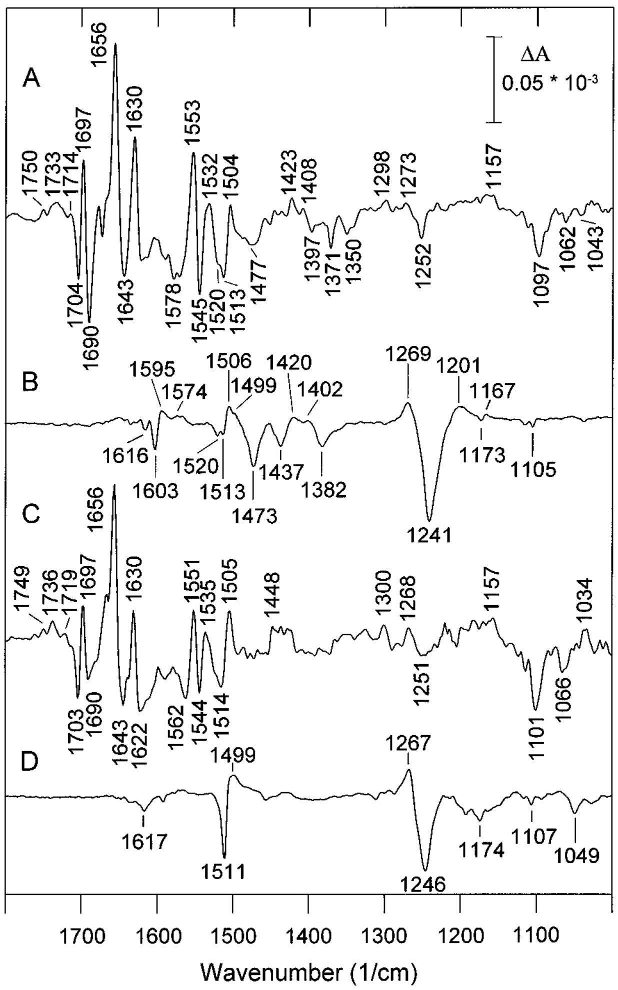

FIGURE 5: $Tyr_D^•/Tyr_D$ spectrum obtained on Tris-washed PS II-enriched membranes (A) at pH 6 in H_2O, 374 400 scans (same as in Figure 4C), and (C) at pD 6 in D_2O, 33 600 scans, compared to cresol•/cresol FTIR difference spectra obtained by a 1 s UV irradiation at 10 K (B) in H_2O at pH 8, 8448 scans, and (D) at pD 8 in D_2O, 6912 scans.

The largest difference bands of the $Tyr_D^•/Tyr_D$ FTIR spectrum (Figures 4C and 5A) are observed at 1656/1643/1630 and 1553/1545 cm^{-1} within the absorption region of the amide I and II modes, respectively. Small reproducible signals are observed, negative at 1513, 1477, 1397, 1371, 1350, and 1252 cm^{-1} and positive at 1504, 1423, 1408, 1298, and 1273 cm^{-1}. The contribution at some of these frequencies of Tyr_D and $Tyr_D^•$ side chain modes, respectively, will be discussed below by comparison with the UV-induced radical-*minus*-non-radical spectrum obtained with cresol (*p*-methylphenol). The $Tyr_D^•/Tyr_D$ FTIR spectrum is further characterized by positive signals at 1733 and 1750 cm^{-1}, a differential signal at 1704/1697 cm^{-1}, and broad signals, positive at ≈1157 cm^{-1} and negative at 1097 cm^{-1} (see Figure 5A).

Figure 5 compares the $Tyr_D^•/Tyr_D$ FTIR difference spectra obtained in H_2O at pH 6 (Figure 5A) and in D_2O at pD 6 (Figure 5C) with the radical-*minus*-non-radical (cresol•/cresol) FTIR difference spectra obtained by UV irradiation of cresol at 10 K in H_2O at pH 8 (Figure 5B) and in D_2O at pD 8 (Figure 5D). The cresol was dissolved in borate buffer, and the radical was formed as described for phenol in (Berthomieu & Boussac, 1995). It was verified by EPR spectroscopy in these experimental conditions that UV irradiation results in electron abstraction and formation of neutral radicals. The absence of contributions from the borate buffer to the UV-induced FTIR difference spectrum is demonstrated, for example, by the shift of all the IR bands of the FTIR spectrum obtained with phenol upon perdeuteration of the phenol ring (Berthomieu & Boussac, 1995).

In the cresol$^•$/cresol FTIR difference spectrum, the negative signals at 1616, 1603, 1520, 1513, 1241, 1173, and 1105 cm^{-1} correspond within a few wavenumbers to frequencies observed for the IR absorption spectrum of cresol (not shown; Jakobsen, 1965; Takeuchi et al., 1988) and are assigned to the υ_{8a}(CC), υ_{8b}(CC), υ_{19a}(CC), and υ_{19b}(CC) ring stretching modes and, υ_{7a}(CO), δ_{9a}(CH), and δ_{15}(CH) modes, respectively [Wilson notation, see Cummings and Wood (1974)]. The negative signals at 1473, 1437, and 1382 cm^{-1} in Figure 5B of cresol in H_2O are not observed for cresol in D_2O (Figure 5D) because they are largely downshifted upon H/D exchange, possibly to 1200−1150 and 1049 cm^{-1}. Therefore, these modes imply COH or OH bending motions (δ) of the cresol hydroxyl, D-labeled upon H_2O/D_2O exchange.

The cresol$^•$/cresol FTIR difference spectra provide the first report of IR modes of cresol$^•$. The two largest positive signals are observed at 1269 and at 1506 cm^{-1}, with a shoulder at 1499 cm^{-1}. Small positive bands are present at 1595, 1574, 1420, 1402, 1201, and 1167 cm^{-1}. The changes observed upon H/D exchange are dominated by effects on the negative bands, in particular in the 1500−1300 cm^{-1} region. The positive band of cresol$^•$ at 1499 cm^{-1} (Figure 5B) is not modified in D_2O (Figure 5D), while the positive signal at 1506 cm^{-1} of cresol$^•$ is not seen in Figure 5D, probably because of overlap with the large negative band of cresol at 1511 cm^{-1} in D_2O.

A number of analogies are observed between spectra A and B in Figure 5. Negative signals at 1520, 1513, and 1252 cm^{-1} in Figure 5A seem to correspond to signals at 1520, 1513, and 1241 cm^{-1} in Figure 5B. In addition, negative bands at 1477, 1371, and 1350 cm^{-1} in Figure 5A, which are absent in the $Tyr_D^•/Tyr_D$ FTIR spectrum in D_2O (Figure 5C), could correspond to the signal at 1473 cm^{-1} and the broad band at 1382 cm^{-1} in the cresol$^•$/cresol FTIR spectrum (Figure 5B), since the latter signals are also absent in the cresol$^•$/cresol FTIR spectrum in D_2O (Figure 5D). The negative signals at 1520, 1513, 1477, 1371, 1350, and 1252 cm^{-1} in Figure 5A are possible candidates for Tyr_D IR modes. Similarly, analogies between positive bands at 1506, 1420, 1402, and 1269 cm^{-1} in the cresol$^•$/cresol spectrum (Figure 5B) and positive ones at 1504, 1423, 1408, and 1273 cm^{-1} in the $Tyr_D^•/Tyr_D$ spectrum (Figure 5B) suggest that $Tyr_D^•$ could contribute at the latter frequencies.

Comparison of the $Tyr_D^•/Tyr_D$ and cresol$^•$/cresol FTIR spectra both in H_2O and in D_2O in Figure 5 also indicates that the largest signals of the $Tyr_D^•/Tyr_D$ FTIR spectrum which are observed above 1620 cm^{-1} do not originate from the tyrosine side chain. This points to the reorganization of the peptide backbone, amino acid side chains, and/or cofactors upon $Tyr_D^•$ formation.

The effect of H/D substitution on the positive signals at 1750−1710 cm^{-1} suggests that a positive signal at ≈1733 cm^{-1} is downshifted to 1719 cm^{-1} in D_2O while two signals at 1750 and 1736 cm^{-1} are not modified (Figure 5C). This is consistent with the possible contribution at ≈1733 cm^{-1} of the protonated side chain of an aspartic or glutamic acid (Chirgadze et al., 1975; Venyaminov & Kalnin, 1990). For experiments performed in the same conditions of illumination and acquisition duration, the ferricyanide and ferrocyanide difference bands give an estimate of the amount of PS II RCs performing charge separation. The two $Tyr_D^•/Tyr_D$ spectra in H_2O and D_2O have been scaled to the same size of the ferricyanide and ferrocyanide difference bands (not shown). The amplitudes of the signals at 1656/1643 cm^{-1} are comparable in the two spectra, while the difference signal at ≈1553/1545 cm^{-1} is two times smaller in the $Tyr_D^•/Tyr_D$ spectrum in D_2O than in H_2O. This effect can be explained by the contribution of amide II mode(s) at these frequencies, which have exchanged for about 50% of the PS II RCs, since the amide II mode is downshifted by ca. 100 cm^{-1} upon H/D exchange (Susi, 1969). The signal at 1448 cm^{-1} in Figure 5C could reveal the corresponding amide II′ band. In contrast to this relatively limited exchange, two signals at 1690 and 1578 cm^{-1} are almost totally absent or downshifted in the $Tyr_D^•/Tyr_D$ spectrum in D_2O.

DISCUSSION

In the present work, experimental conditions leading to the generation of pure Q_A^-/Q_A or $Tyr_D^•/Tyr_D$ FTIR difference spectra have been optimized. Excitation by single-turnover flash or short illumination of samples in the presence of an exogenous reductant or oxidant was used. These procedures allow the study of a single radical species and prevents the photoaccumulation of undesired light-induced states that could be generated under continuous illumination. The Q_A^- and $Tyr_D^•$ radicals were formed with high yield and a lifetime of several seconds or minutes allowing the averaging of the FTIR difference spectra with high signal to noise ratio.

Primary Quinone Acceptor Q_A. The first Q_A^-/Q_A spectrum was reported in Berthomieu et al. (1990) on spinach PS II-enriched membranes in the presence of NH_2OH and DCMU. A Q_A^-/Q_A FTIR spectrum with improved signal to noise ratio was later obtained by the addition of PMS as electron acceptor from Q_A^- in the presence of DCMU (Berthomieu et al., 1992a). In the present work, we show the EPR spectra recorded in the same experimental conditions as for the Q_A^-/Q_A FTIR spectrum. The EPR signals observed at $\mathbf{g} \approx 2$ correspond to the reduced PMS^- radical. This radical is present already in the dark-adapted sample, and its concentration increases only marginally upon illumination. This is shown by the comparison of the light-induced EPR difference spectrum at $\mathbf{g} \approx 2$ with the $Tyr_D^•$ EPR signal measured on a Tris-washed sample with the same PS II RC concentration (Figure 3C). The light-induced signal is also distinctly different from and much smaller than the Chl^+ EPR signal expected if this species would be photoaccumulated in 5% of the PS II centers. Therefore, it can be concluded that no detectable Chl^+ EPR signal (i.e., less than even 1%) is observed upon illumination of the sample in the conditions used to record the FTIR data. The EPR controls also demonstrate that the primary electron acceptor Q_A is photoreduced for about 40% of PS II centers and is detectable after a short illumination at 10 °C. Therefore the FTIR difference spectrum presented here is denoted as a Q_A^-/Q_A spectrum and is discussed as contributions from the photoreduction of the quinone itself and from the amino acids or other cofactors influenced by the accumulation of a negative charge on Q_A. The Q_A^-/Q_A FTIR spectrum is characterized by a differential signal at 1724/1719 cm^{-1} and its largest positive band at 1478 cm^{-1} in spinach PS II-enriched membranes. An identical Q_A^-/Q_A spectrum has also been obtained in the presence of NH_2OH and DCMU by Noguchi et al. (1992), and a similar spectrum was reported by Araga et al. (1993). The diagnostic band at 1478 cm^{-1} is present in the $S_2Q_A^-/S_1Q_A$ (Noguchi et al., 1992) and in the two Cytb559ox Q_A^-/Cytb559red Q_A spectra recorded at low temperature (Berthomieu et al., 1992b; Noguchi et al., 1993a). In these experimental conditions, charge separation occurred between the primary electron acceptor Q_A and different electron donors to P_{680}. Therefore, common IR spectral features in these spectra are assigned to the photoreduction of Q_A.

Recently, MacDonald et al. (1995) obtained a spectrum very similar to the Q_A^-/Q_A spectrum reported in Figure 4A. This spectrum was however interpreted as dominated by Chl^+/Chl contributions. In particular, the positive band at 1478 cm^{-1} was assigned to a Chl^+ mode. In contrast to our experimental procedure (flash or short illumination at 10 °C on samples with NH_2OH, PMS, and DCMU), MacDonald et al. (1995) recorded the IR spectra under continuous illumination (more than 5 min) at −9 °C on PS II-enriched membranes in the presence of NH_2OH and ferricyanide. EPR control experiments at $\mathbf{g} = 2$ in these particular conditions were taken as indicative that a chlorophyll radical was reversibly photoaccumulated for ≈3% or 6% of the PS II centers, when 8 or 90 min dark adaptation was used between successive illuminations, respectively. On the basis of Chl^+ detection by EPR, the largest bands of the FTIR difference spectra were interpreted as Chl^+/Chl contributions. However, no EPR experiments were performed on the samples to measure the amount of Q_A^- that was photoaccumulated in these conditions. The influence of the dark adaptation period on the concentration of Q_A^- is therefore unknown (MacDonald et al., 1995). In the absence of these controls, it is not possible to determine the nature of the dominant photoaccumulated species. Actually, the FTIR difference signals are only about 1.2 times larger with 90 min dark adaptation between illuminations than with 8 min, whereas the Chl^+ EPR signal is 2 times larger (MacDonald et al., 1995). This argues that Chl^+ is not the only species seen in the FTIR spectra and that the largest IR signals are not due to Chl^+. The influence of dark adaptation duration on the FTIR difference signals reflects more likely the reoxidation kinetic of Q_A^- by ferricyanide than the reduction of Chl^+. The absence of signals upon cyclic illumination of PS II samples in the presence of NH_2OH and in the absence of any exogenous electron acceptor (MacDonald et al., 1995) could be explained by the irreversible photoreduction of Q_A that could occur already under dim green light during sample preparation.

In addition, light-induced FTIR difference spectra recorded with a Mn-depleted PS II core preparation of spinach in the presence of ferricyanide or ferrocyanide in MacDonald and Barry (1992) present large analogies with spectra obtained by the same group with samples in the presence of NH_2OH (MacDonald et al., 1995) as well as with the Q_A^-/Q_A spectrum presented here. This is illustrated, for example, by the differential signal at 1724/1718 cm^{-1} and the positive band at 1478 cm^{-1}. The EPR control experiments corresponding to the FTIR difference spectrum obtained with samples in the presence of ferrocyanide alone in MacDonald and Barry (1992) show that no Chl^+ is photoaccumulated in these conditions. This further argues that the 1478 cm^{-1} signal cannot be assigned to a Chl^+ mode. No control of the amount of Q_A photoreduction was reported in this study aiming at the detection of $Tyr_D^\bullet$ and $Tyr_Z^\bullet$ modes. However, in the presence of ferrocyanide, Q_A^- photoaccumulation can be expected to occur very efficiently upon illumination at −9 °C for a large majority of PS II centers.

An argument presented against the assignment of the 1478 cm^{-1} band to an IR signal of the Q_A^- state was that this signal is observed in samples without DCMU (MacDonald et al., 1995), which blocks the electron transfer from Q_A^- to Q_B. However, in their study, the authors did not present any evidence for functional electron transfer from Q_A^- to Q_B in the dried samples used for the FTIR experiments. Another argument against the assignment of the signal at 1478 cm^{-1} to a mode of Q_A^- was that this signal is downshifted by 2 cm^{-1} upon ^{15}N-labeling in *Synechocystis* sp. PCC 6803 PS II (MacDonald et al., 1995), while the quinone modes should be insensitive to ^{15}N-labeling. We propose that the 1478 cm^{-1} signal may correspond to the $\nu(C{\cdots}O)$ mode of Q_A^- because no shift of this signal is observed in the Q_A^-/Q_A spectrum recorded with ^{15}N-labeled spinach PS II (Berthomieu et al., 1992a) (Figure 4A,B). The discrepancy between data in Berthomieu et al. (1992a) and MacDonald et al. (1995) was explained by the latter authors by the assumption that we only obtained low levels of ^{15}N-incorporation in the spinach PS II membranes. However, ESEEM experiments performed on the same ^{15}N-labeled spinach preparation indicated an extent of labeling of at least 85% (Deligiannakis et al., 1995). This high extent of labeling is also illustrated by the downshift of 15 cm^{-1} upon ^{15}N-labeling (Figure 4B) observed for all of the signals at 1560/1550/1542 cm^{-1} in ^{14}N-labeled samples (Figure 4A). The ^{15}N-induced downshift indicates that peptide $\nu(CN) + \delta(NH)$ vibrations contribute at these frequencies. In this spectral region, our Q_A^-/Q_A spectrum is indeed very similar to the spectrum observed by MacDonald et al. (1995). In addition, the signals at 1682 and 1672 cm^{-1} in Figure 4A are reproducibly downshifted by 2 cm^{-1} upon ^{15}N-labeling (Figure 4B). Therefore, we are confident that the 1478 cm^{-1} band is not modified by the ^{15}N-labeling within the ±1 cm^{-1} accuracy of the method. The 2 cm^{-1} downshift of the positive band at 1478 cm^{-1} observed upon ^{15}N-labeling in spectra recorded with *Synechocystis* sp. PCC 6803 in MacDonald et al. (1995) was used as a demonstration that this band corresponds mainly to a Chl^+ mode. However, it should be noted that an IR mode in this region has only been reported upon photooxidation of the primary electron donor of bacterial photosynthetic RC, which is a bacteriochlorophyll (BChl) dimer (Mäntele et al., 1988). No signal was observed in this region in the Chl^+/Chl or $BChl^+/BChl$ FTIR difference spectra generated by electrochemistry (Mäntele et al., 1988; Leonhard et al., 1989; Nabedryk et al., 1990) upon Chl^+ formation in PS II (Noguchi & Inoue, 1995b; unpublished data), or upon photoxidation of the primary electron donor P_{700} of PS I (MacDonald et al., 1993; Nabedryk et al., 1990; Tavitian et al., 1986). From the EPR control experiments presented here, we assign the whole band at 1478 cm^{-1} to the Q_A^- state. However, the small shift reported in the study of *Synechocystis* sp. PCC 6803 could indicate that two different contributions are superimposed at 1478 cm^{-1}, a small one from protein side chain mode(s), downshifted upon

^{15}N-labeling, and the dominant one from the semiquinone ν(C⋯O) mode.

Finally, continuous illumination of dried samples at −9 °C can indeed cause $\mathrm{Chl^+}$ accumulation in a small fraction of PS II centers. Comparison of spectra in MacDonald et al. (1995) and in Figure 4A, which differ by the 3−6% $\mathrm{Chl^+/Chl}$ contribution present only in the spectra of MacDonald et al. (1995), suggests that the $\mathrm{Chl^+/Chl}$ signals are marginal and responsible for the small spectral differences between the two spectra, notably in the 1750−1650 $\mathrm{cm^{-1}}$ region (MacDonald et al., 1995). Indeed, the most intense IR modes of a $\mathrm{Chl^+/Chl}$ FTIR difference spectrum are expected to contribute in this spectral region (Nabedryk et al., 1990).

The proper assignment of the $\mathrm{Q_A^-/Q_A}$ FTIR difference signals is essential for the investigation of the IR modes of tyrosine or chlorophyll oxidation. In fact, interpretation of IR modes from both $\mathrm{Tyr_D}$ and $\mathrm{Tyr_Z}$ in MacDonald et al. (1992) and Bernard et al. (1995) may be complicated by the presence in their spectra of substantial contribution of $\mathrm{Q_A^-/Q_A}$ IR signals. We have developed a different approach to obtain the $\mathrm{Tyr_D^\bullet/Tyr_D}$ FTIR difference spectra free from other contributions.

Tyrosine D. The $\mathrm{Tyr_D^\bullet/Tyr_D}$ FTIR spectrum is recorded on Tris-washed PS II membranes from spinach at pH 6 in the presence of phosphate, formate, and ferricyanide. EPR experiments performed on these samples at both the $\mathrm{Tyr^\bullet}$ and $\mathrm{Q_A^-{-}Fe^{2+}}$ EPR signals have shown that it is possible to optimize experimental conditions to record the FTIR difference spectrum only due to $\mathrm{Tyr_D}$ photooxidation. The absence of contributions from the electron acceptor side is also shown by the ferrocyanide and ferricyanide IR signals and the absence of analogies between the $\mathrm{Tyr_D^\bullet/Tyr_D}$ and the $\mathrm{Q_A^-/Q_A}$ FTIR difference spectra (Figure 4). The $\mathrm{Tyr_D^\bullet/Tyr_D}$ FTIR spectrum shows the vibrational differences due to $\mathrm{Tyr_D}$ itself and to amino acids and cofactors of its environment. The contributions of $\mathrm{Tyr_D}$ and $\mathrm{Tyr_D^\bullet}$ are studied by comparison with the $\mathrm{cresol^\bullet/cresol}$ FTIR difference spectrum obtained by UV irradiation at 10 K.

Resonance Raman (RR) spectroscopy has been used previously to study radicals of (substituted) phenols obtained at room temperature either chemically (Tripathi & Schuler, 1984, 1988) or by UV irradiation (Beck & Brus, 1982; Johnson et al., 1986; Mukherjee et al., 1995). Recently, the effect of ^{17}O- and ^{13}C-labeling was studied on the RR spectra of UV-induced phenoxyl radical (Mukherjee et al., 1995). However, the selection rules are not the same for RR and IR spectroscopies. This is illustrated by the differences between the RR and IR spectra of tyrosine (Ames et al., 1992; Dollinger et al., 1986). Three modes are principally enhanced at 1615, 1206, and 1174 $\mathrm{cm^{-1}}$ by RR, while the largest IR bands are found at 1518 and 1248 $\mathrm{cm^{-1}}$ (1499 and 1269 $\mathrm{cm^{-1}}$ for tyrosinate). The same differences are also observed for cresol (Ames et al., 1992; Takeuchi et al., 1988). This motivated the investigation of IR modes of the radicals of tyrosine and models of its side chain: phenol and *p*-ethylphenol by UV-induced FTIR difference spectroscopy at 10 K (Berthomieu & Boussac, 1995). Common signals are observed by IR and RR for the phenoxyl radical at 1556−1552, 1515−1503, and 1167−1157 $\mathrm{cm^{-1}}$. Two additional modes are observed by FTIR spectroscopy at ≈1500 and 1290−1270 $\mathrm{cm^{-1}}$, while the RR bands at 1398−1393 $\mathrm{cm^{-1}}$ (Beck & Brus, 1982; Johnson et al., 1986; Muckherjee et al., 1995) and 1331 $\mathrm{cm^{-1}}$ [only observed in Tripathi and Schuler (1984)] are not detected in IR (Berthomieu & Boussac, 1995). In particular, analogous downshifts upon uniform D-labeling were reported by IR and RR for the signal of the phenoxyl radical at 1505 $\mathrm{cm^{-1}}$. It was shown by UV-RR that this mode is sensitive to ^{17}O-labeling (Muckherjee et al., 1995). A downshift of this mode is also observed in IR spectra upon ^{18}O-labeling (A. Boussac, C. Berthomieu, and C. Boullais, unpublished). Therefore, the same mode is observed in IR and RR at ≈1505 $\mathrm{cm^{-1}}$ which is assigned to the ν(CO) mode of the phenoxyl radical. For the radicals of tyrosine, *p*-ethylphenol, and cresol, this mode is observed between 1515 and 1504 $\mathrm{cm^{-1}}$ in IR (Berthomieu & Boussac, 1995).

Cresol revealed the best model for detecting the IR signals of the tyrosine side chain in PS II, since the IR modes of cresol are within a few wavenumbers of those of the tyrosine side chain in solution (Dollinger et al., 1986; Takeuchi et al., 1988). Cresol is also soluble at pH below its $\mathrm{p}K_\mathrm{a}$, while tyrosine is hardly soluble below its $\mathrm{p}K_\mathrm{a}$. In addition, differential IR signals from the Tyr amino acid function overlap with those from the phenolic side chain in the UV-induced $\mathrm{Tyr^\bullet/Tyr}$ FTIR difference spectra (Berthomieu & Boussac, 1995).

$\mathrm{Cresol^\bullet/cresol}$ FTIR spectra were obtained at pH 8 and 12, i.e., below and above the $\mathrm{p}K_\mathrm{a}$ of cresol. The spectra differ essentially by the frequencies of cresolate at 1504 and 1270 $\mathrm{cm^{-1}}$ or cresol at 1520−1513 and 1241 $\mathrm{cm^{-1}}$ (not shown). For cresol in solution, three additional bands are observed at 1473, 1437, and 1382 $\mathrm{cm^{-1}}$, which are largely downshifted in $\mathrm{D_2O}$ (Figure 5). The $\mathrm{Tyr_D^\bullet/Tyr_D}$ FTIR spectrum compares better with the $\mathrm{cresol^\bullet/cresol}$ spectrum obtained at pH 8 (Figure 5). Similarities between the $\mathrm{cresol^\bullet/cresol}$ and $\mathrm{Tyr_D^\bullet/Tyr_D}$ spectra suggest that the ring ν(CC) and ν(CO) modes of the $\mathrm{Tyr_D}$ side chain contribute at 1513 and 1252 $\mathrm{cm^{-1}}$, respectively, and that signals at 1477, 1371, and 1350 $\mathrm{cm^{-1}}$ could also be due to $\mathrm{Tyr_D}$. The frequencies of the ring vibrations provide an experimental evidence that reduced $\mathrm{Tyr_D}$ is protonated (Dollinger et al., 1986). At ≈1615−1603 $\mathrm{cm^{-1}}$, the tyrosine signals probably overlap with other protein modes.

The largest IR modes of $\mathrm{cresol^\bullet}$ at pH 8 are observed at 1506, 1420, and 1269 $\mathrm{cm^{-1}}$ (Figure 5B). At pH 12, the 1269 $\mathrm{cm^{-1}}$ signal is replaced by a larger band at 1285 $\mathrm{cm^{-1}}$ (not shown). This pH effect was also observed for a band at 1275 or 1290 $\mathrm{cm^{-1}}$ for the phenoxyl radical at pH 8 or 12, respectively (Berthomieu & Boussac, 1995). Comparison of the $\mathrm{Tyr_D^\bullet/Tyr_D}$ spectrum with the UV-induced $\mathrm{cresol^\bullet/cresol}$ FTIR spectrum suggests that the $\mathrm{Tyr_D^\bullet}$ side chain contributes at 1504 $\mathrm{cm^{-1}}$ in PS II and, possibly, also at 1423 and 1273 $\mathrm{cm^{-1}}$.

The comparison between the $\mathrm{Tyr_D^\bullet/Tyr_D}$ and $\mathrm{cresol^\bullet/cresol}$ FTIR difference spectra reveals that a large number of signals, and notably the largest ones, are not contributed by the $\mathrm{Tyr_D}$ side chain. The largest bands observed at 1656/1643 and 1553/1545 $\mathrm{cm^{-1}}$ could be due to amide I and II modes of the protein backbone and may reflect changes in the hydrogen bonding or polarization of peptide carbonyls. A part of the complex positive signal at 1733−20 $\mathrm{cm^{-1}}$ in the $\mathrm{Tyr_D^\bullet/Tyr_D}$ spectrum, modified upon H/D exchange, could be explained by the protonation of Asp or Glu residue(s) upon $\mathrm{Tyr_D}$ radical formation. Since Asp and Glu residues are not present in the models of the immediate environment of $\mathrm{Tyr_D}$ (Svensson et al., 1990; Svensson, 1995), either the occurrence of a long range charge effect or the implication of another polypeptide docking onto the Tyr_D environment can be postulated. A sharp differential signal is observed at 1703/1697 cm^{-1} in the $Tyr_D^•/Tyr_D$ FTIR spectrum. This signal, not modified upon H/D exchange, could correspond to a free peptide carbonyl group. However, the high frequency of this signal favors its assignment to the 9-keto carbonyl of a neutral Chl [Nabedryk et al. (1990) and references therein]. Indeed, an electrochromic shift at ≈432 nm of a chlorophyll electronic transition—possibly from P_{680}—has been observed upon $Tyr_D^•$ formation (Diner et al., 1995). A negative signal at 1690 cm^{-1} in the $Tyr_D^•/Tyr_D$ FTIR spectrum (Figure 5A), probably downshifted to 1622 cm^{-1} upon H/D exchange (Figure 5C), could be due to the side chain mode of an arginine residue (Venyaminov & Kalnin, 1990).

The broad signals positive at ≈1157 cm^{-1} and negative at 1097 cm^{-1} most probably arise from phosphate ν(PO) modes of $H_2PO_4^{2-}$ and HPO_4^{3-}, respectively (Chapman & Thirwell, 1964). These bands indicate that the protonation of a phosphate group of the buffer occurs upon $Tyr_D^•$ formation. Changes in phosphate IR bands due to proton release have been reported upon electrochemical reduction of various cytochrome *c*1 (Baymann, 1995) and also observed upon the non-heme iron oxidation in PS II (R. Hienerwadel, unpublished). The signals at ≈1157 and 1097 cm^{-1} in Figure 5A indicate that proton release at the PS II membrane surface occurs upon $Tyr_D^•$ formation.

The $Tyr_D^•/Tyr_D$ spectrum presented here is very different from spectra in the literature where Tyr_D and $Tyr_D^•$ were expected to contribute (MacDonald & Barry, 1992; MacDonald et al., 1993). As explained above, the latter spectra exhibit similarities with the Q_A^-/Q_A FTIR spectrum and spectra obtained with samples incubated with NH_2OH (MacDonald et al., 1995) which reduces very efficiently $Tyr_D^•$ and $Tyr_Z^•$. This suggests that the contributions from Tyr_D or Tyr_Z in the spectra by MacDonald and Barry (1992) are masked by the Q_A^-/Q_A signals. In this work (MacDonald & Barry, 1992), light-*minus*-dark FTIR difference spectra were recorded on dehydrated spinach PS II core complexes illuminated at −9 °C in the presence of either ferricyanide or ferrocyanide. EPR control at $\mathbf{g} \approx 2$ showed that $Tyr_Z^•$ and Chl^+ were photoaccumulated under illumination in the sample with ferricyanide, while only $Tyr_D^•$ was accumulated in the photosteady state at the electron donor side of PS II in the sample with ferrocyanide. However, the FTIR difference spectra obtained for the two samples were very similar. In order to cancel contributions from Q_A^-/Q_A signals, interactive subtraction was done between FTIR difference spectra obtained in the PS II samples with ferricyanide or ferrocyanide. The size of the amide II mode in the absorption spectra of the different IR samples was used to quantify the RC concentration of each sample (MacDonald & Barry, 1992). However, this procedure did not take into account that different amounts of charge separation most probably occurred in the PS II samples with ferricyanide or ferrocyanide. Since this subtraction procedure does not take into account the different amounts of charge separation, it will not cancel the Q_A^-/Q_A contributions completely.

In the study by MacDonald et al. (1993), signals at 1477 and 1473 cm^{-1} were assigned to the ν(CO) mode of $Tyr_Z^•$ and $Tyr_D^•$, respectively, by the comparison of spectra obtained with PS II core samples of *Synechocystis* sp. PCC 6803 with unlabeled, ^{2}H-labeled, or ^{13}C-labeled tyrosines. However, intensity changes rather than clear frequency downshifts of the IR signals were observed upon tyrosine labeling so that uncertainty remains whether these signals are properly assigned to the reduced or radical state, respectively. They could also be due to slight variations from one spectrum to the other of the IR contributions from contaminant P_{700}^+/P_{700} (10% PS I contamination is reported by the authors) and Q_A^-/Q_A signals. Large contributions of P_{700} signals in the 1300−1200 cm^{-1} region did not allow the detection of the ν(CO) mode of neutral Tyr_Z or Tyr_D expected between 1270 and 1240 cm^{-1} (MacDonald et al. 1993). Finally, the spectrum in MacDonald et al., (1993) presents strong analogies with a temperature-induced FTIR difference spectrum generated upon increasing by 1 °C the temperature of a sample of PS II-enriched membranes (Noguchi et al., 1993b). Notably, a large negative band at 1562 cm^{-1}, followed by a broad positive band at 1540−1480 cm^{-1}, and negative bands at ≈1630 and ≈1470 cm^{-1} seem common to both spectra. This similarity suggests that heating of the sample by the actinic beam has probably taken place in the spectra reported by MacDonald et al. (1993).

The ν(CO) mode of the radicals of tyrosine, *p*-ethylphenol, and cresol is always observed above 1500 cm^{-1} in both RR and IR studies (Beck & Brus, 1982; Berthomieu & Boussac, 1995; Johnson et al., 1986; Mukherjee et al., 1995; Tripathi & Schuler, 1984, 1988). The ν(CO) mode of the $Tyr^•$ present in ribonucleotide reductase has been reported at 1498 cm^{-1} by RR (Backes et al., 1989). This $Tyr^•$ is not hydrogen bonded (Nordlund et al., 1990). MacDonald et al. (1993) explained the low frequency (1473 cm^{-1}) proposed for the ν(CO) mode of $Tyr_D^•$ by the presence of a hydrogen bond. However, there is no evidence that the mode observed at 1505 cm^{-1} in RR and IR is downshifted upon formation of a hydrogen bond. In contrast to the data reported by MacDonald et al. (1993), no positive signal is observed at 1478−1470 cm^{-1} in the $Tyr_D^•/Tyr_D$ FTIR spectrum presented here. A broad negative signal is centered at 1477 cm^{-1} in this spectral range (Figure 5A). The comparison with the UV-induced cresol$^•$/cresol FTIR spectrum suggests that the $Tyr_D^•$ side chain contributes at 1504 cm^{-1}.

In conclusion, the $Tyr_D^•/Tyr_D$ spectrum presented in this work provides the basis for the detailed study of Tyr_D and its environment. This study is underway in collaboration with X.-S. Tang and B. Diner (DuPont de Nemours, Wilmington, DE) through the use of wild type, specifically labeled, and mutant PS II of *Synechocystis* sp. PCC 6803.

ACKNOWLEDGMENT

Eliane Nabedryk is acknowledged for discussions and reading the manuscript and Bruce Diner for discussions.

REFERENCES

Ames, J. B., Ros, M., Raap, J., Lugtenburg, J., & Mathies, R. A. (1992) *Biochemistry 31*, 5328−5334.

Araga, C., Akabori, K., Sasaki, J., Maeda, A., Shiina, T., & Toyoshima, Y. (1993) *Biochim. Biophys. Acta 1142*, 36−42.

Babcock, G. T., & Sauer, K. (1973) *Biochim. Biophys. Acta 325*, 483−503.

Backes, G., Sahlin, M., Sjöberg, B.-M., Loehr, T. M., & Sanders-Loehr, J. (1989) *Biochemistry 28*, 1923−1929.

Barry, B. A., & Babcock, G. T. (1987) *Proc. Natl. Acad. Sci. U.S.A. 84*, 7099−7103.

Barry, B. A., ElDeeb, M. K., Sandusky, P. O., & Babcock, G. T. (1990) *J. Biol. Chem. 265*, 20139−20143.

Baymann, F. (1995) Doctoral Thesis, University of Freiburg, Germany.

Beck, S. M., & Brus, L. E. (1982) *J. Chem. Phys. 176*, 4700−4704.

Bernard, M. T., MacDonald, G. M., Nguyen, A. P., Debus, R. J., & Barry, B. A. (1995) *J. Biol. Chem. 270*, 1589−1594.

Berthomieu, C. (1991) Doctoral Thesis, University of Paris VI, France.

Berthomieu, C., & Boussac, A. (1995) *Biospectroscopy 1*, 187−206.

Berthomieu, C., Nabedryk, E., Mäntele, W., & Breton, J. (1990) *FEBS Lett. 269*, 363−367.

Berthomieu, C., Nabedryk, E., Breton, J., & Boussac, A. (1992a) in *Research in Photosynthesis* (Murata, N., Ed.) Vol. II, pp 53−56, Kluwer Academic Publishers, Dordrecht, The Netherlands.

Berthomieu, C., Boussac, A., Mäntele, W., Breton, J., & Nabedryk, E. (1992b) *Biochemistry 31*, 11460−11471.

Bögershausen, O., & Junge, W. (1995) *Biochim. Biophys. Acta 1230*, 177−185.

Boussac, A., & Etienne, A.-L. (1982a) *FEBS Lett. 148*, 113−116.

Boussac, A., & Etienne, A.-L. (1982b) *Biochem. Biophys. Res. Comm. 109*, 1200−1205.

Boussac, A., & Etienne, A.-L. (1984) *Biochim. Biophys. Acta 766*, 576−581.

Buser, C. A., Diner, B. A., & Brudwig, G. W. (1992) *Biochemistry 31*, 11441−11448.

Chapman, A. C., & Thirwell, L. E. (1964) *Spectrochim. Acta 20*, 937−947.

Chirgadze, Y. N., Federov, O. V., & Trushina, N. P. (1975) *Biopolymers 14*, 679−694.

Cummings, D. L., & Wood, J. L. (1974) *J. Mol. Struct. 20*, 1−40.

Debus, R. J. (1992) *Biochim. Biophys. Acta 1102*, 269−352.

Debus, R. J., Barry, B. A., Babcock, G. T., & MacIntosh, L. (1988a) *Proc. Natl. Acad. Sci. U.S.A. 85*, 427−430.

Debus, R. J., Barry, B. A., Sithole, I., Babcock, G. T., & MacIntosh, L. (1988b) *Biochemistry 27*, 9071−9074.

Dekker, J. P., van Gorkom, H. J., Bork, M., & Ouwehand, L. (1984) *Biochim. Biophys. Acta 764*, 301−309.

Deligiannakis, Y., Petrouleas, V., & Diner, B. A. (1994) *Biochim. Biophys. Acta 1188*, 260−270.

Deligiannakis, Y., Boussac, A., & Rutherford, A. W. (1995) *Biochemistry 34*, 16030−16038.

Diner, B. A., & Babcock, G. T. (1996) in *Oxygenic Photosynthesis: The Light Reactions* (Ort, D., & Yocum, C., Eds.) pp 213−247, Kluwer Academic Publishers, Dordrecht, The Netherlands.

Diner, B. A., Nixon, P. J., & Farchaus, J. W. (1991) *Curr. Opin. Struct. Biol. 1*, 546−554.

Diner, B. A., Tang, X.-S., Zheng, M., Dismukes, G. C., Force, D. A., Randall, D. W., & Britt, R. D. (1995) in *Photosynthesis: from Light to Biosphere* (Mathis, P., Ed.) Vol. II, 229−234, Kluwer Academic Publishers, Dordrecht, The Netherlands.

Dollinger, G., Eisenstein, L., Lin, S.-L., Nakanishi, K., & Termini, J. (1986) *Biochemistry 25*, 6524−6533.

Evelo, R. G., Hoff, A. J., Dikanov, S. A., & Tyrishkin, A. M. (1989) *Chem. Phys. Lett. 161*, 479−484.

Force, D. A., Randall, D. W., Britt, R. D., Tang, X.-S., & Diner, B. A. (1995) *J. Am. Chem. Soc. 117*, 12643−12644.

Gilchrist, M. L., Ball, J. A., Randall, D. W., & Britt, R. D. (1995) *Proc. Natl. Acad. Sci. U.S.A. 92*, 9545−9549.

Hienerwadel, R., & Berthomieu, C. (1995) *Biochemistry 34*, 16288−16297.

Hienerwadel, R., Boussac, A., & Berthomieu, C. (1993) in *Fifth International Conference on the Spectroscopy of Biological Molecules* (Theophanides, T., et al., Eds.) pp 317−318, Kluwer Academic Publishers, Dordrecht, The Netherlands.

Hienerwadel, R., Boussac, A., Breton, J., & Berthomieu, C. (1995a) in *Spectroscopy of Biological Molecules* (Merlin, J. C., et al., Eds.) pp 193−196, Kluwer Academic Publishers, Dordrecht, The Netherlands.

Hienerwadel, R., Boussac, A., Breton, J., & Berthomieu, C. (1995b) in *Photosynthesis: from Light to Biosphere* (Mathis, P., Ed.) Vol. I, pp 747−750, Kluwer Academic Publishers, Dordrecht, The Netherlands.

Hoganson, C. W., & Babcock, G. T. (1994) in *Metal Ions in Biological Systems* (Sigel, H., & Sigel, A., Eds.) Vol. 30, pp 77−107, Marcel Dekker, New-York.

Hoganson, C. W., Lydakis-Simantiris, N., Tang, X.-T., Tommos, C., Warncke, K., Babcock, G. T., Diner, B. A., McCraken, J., & Styring, S. (1995) *Photosynth. Res. 46*, 177−184.

Ikegami, I., & Katoh, S. (1973) *Plant Cell Physiol. 14*, 829−836.

Jakobsen, R. J. (1965) *Spectrochim. Acta 21*, 433−442.

Johnson, C. R., Ludwig, M., & Asher, S. A. (1986) *J. Am. Chem. Soc. 108*, 905−912.

Leonhard, M., Wollenweber, A., Berger, G., Kléo, J., Nabedryk, E., Breton, J., & Mäntele, W. (1989) in *Techniques and New Developments in Photosynthesis Research* (Barber, J., & Malkin, R., Eds.) NATO ASI Series, Vol. 168, pp 115−118, Plenum, New York.

MacDonald, G. M., & Barry, B. A. (1992) *Biochemistry 31*, 9848−9856.

MacDonald, G. M., Bixby, K. A., & Barry, B. A. (1993) *Proc. Natl. Acad. Sci. U.S.A. 90*, 11024−11028.

MacDonald, G. M., Steenhuis, J. J., & Barry, B. A. (1995) *J. Biol. Chem. 270*, 8420−8428.

Mäntele, W. (1993) *Trends Biochem. Sci. 18*, 197−202.

Mäntele, W., Wollenweber, A., Nabedryk, E., & Breton, J. (1988) *Proc. Natl. Acad. Sci. U.S.A. 85*, 8468−8472.

Metz, J. G., Nixon, P. J., Rögner, M., Brudwig, G. W., & Diner, B. A. (1989) *Biochemistry 28*, 6960−6969.

Michel, H., & Deisenhofer, J. (1988) *Biochemistry 27*, 1−7.

Mino, H., Satoh, J.-I., Kawamori, A., Toriyama, K., & Zimmerman, J.-L. (1993) *Biochim. Biophys. Acta 1144*, 426−433.

Mukherjee, A., McGlashen, M. L., & Spiro, T. G. (1995) *J. Phys. Chem. 99*, 4912−4917.

Nabedryk, E., Leonhard, M., Mäntele, W., & Breton, J. (1990) *Biochemistry 29*, 342−3247.

Noguchi, T., & Inoue, Y. (1995a) *J. Biochem.* (*Tokyo*) *118*, 9−12.

Noguchi, T., & Inoue, Y. (1995b) *FEBS Lett. 370*, 241−244.

Noguchi, T., Ono, T., & Inoue, Y. (1992) *Biochemistry 31*, 5953−5956.

Noguchi, T., Ono, T., & Inoue, Y. (1993a) *Biochim. Biophys. Acta 1143*, 333−336.

Noguchi, T., Inoue, Y., & Satoh, K. (1993b) *Biochemistry 32*, 7186−7195.

Nordlund, P., Sjöberg, B.-M., & Eklund, H. (1990) *Nature 345*, 593−598.

Petrouleas, V., & Diner, B. A. (1986) *Biochim. Biophys. Acta 849*, 264−275.

Renger, G., & Völker, M. (1982) *FEBS Lett. 149*, 203−207.

Rodriguez, I. D., Chandrashekar, T. K., & Babcock, G. T. (1987) in *Progress in Photosynthesis Research* (Biggins, J., Ed.) pp 471−474, Martinus Nijhoff, Dordrecht, The Netherlands.

Roffey, R. A., vanWijk, K. J., Sayre, R. T., & Styring, S. (1994) *J. Biol. Chem. 269*, 5115−5121.

Rutherford, A. W. (1989) *Trends Biochem. Sci. 14*, 227−232.

Rutherford, A. W., & Zimmernann, J. L. (1984) *Biochim. Biophys. Acta 767*, 168−175.

Ruffle, S. V., Donnelly, D., Blundell, T. L., & Nugent, J. H. A. (1992) *Photosynth. Res. 34*, 287−300.

Sun, U., Tang, X.-S., & Diner, B. (1996) *Biochemistry 35*, 679−684.

Susi, H. (1969) in *Structure and Stability of Biological Macromolecules* (Tunasheff, S. N., & Fasman, G. D., Eds.) Vol. 2, pp 575−663, Dekker, New York.

Svensson, B. (1995) Doctoral Thesis, Stockholm University, Sweden.

Svensson, B., Vass, I., Cedergren, E., & Styring, S. (1990) *EMBO J. 7*, 2051−2059.

Takeuchi, H., Watanabe, N., & Harada, I. (1988) *Spectrochim. Acta 44A*, 749−761.

Tang, X.-S., Chrisholm, D. A., Dismukes, G. C., Brudwig, G. W., & Diner, B. A. (1993) *Biochemistry 32*, 13742−13748.

Tang, X.-S., Zheng, M., Chrisholm, D. A., Dismukes, G. C., & Diner, B. (1996) *Biochemistry 35*, 1475−1484.

Tavitian, B. A., Nabedryk, E., Mäntele, W., & Breton, J. (1986) *FEBS Lett. 201*, 151−157.

Tommos, C., Davidson, L., Svensson, B., Madsen, C., Vermaas, W. F. J., & Styring, S. (1993) *Biochemistry 32*, 5436−5441.

Tommos, C., Tang, X.-S., Warncke, K., Hoganson, C. W., Styring, S., McCracken, J., Diner, B. A., & Babcock, G. T. (1995) *J. Am. Chem. Soc. 117*, 10325−10335.

Tripathi, G. N. R., & Schuler, R. H. (1984) *J. Chem. Phys. 81*, 113−121.

Tripathi, G. N. R., & Schuler, R. H. (1988) *J. Phys. Chem. 92*, 5129−5133.

Vass, I., & Styring, S. (1991) *Biochemistry 30*, 830−839.

Vass, I., Deak, Z., & Hideg, E. (1990) *Biochim. Biophys. Acta 1017*, 63−69.

Venyaminov, S. Y., & Kalnin, N. N. (1990) *Biopolymers 30*, 1243−1257.

Vermaas, W. F. J., & Rutherford, A. W. (1984) *FEBS Lett. 175*, 243−248.

Vermaas, W. F. J., Rutherford, A. W., & Hansson, O. (1988) *Proc. Natl. Acad. Sci. U.S.A. 85*, 8477−8481.

Zimmerman, J. L., Boussac, A., & Rutherford, A. W. (1993) *Biochemistry 32*, 4831−4841.

BI961952D